Journal of Asian Earth Sciences 54–55 (2012) 72–77

Contents lists available at SciVerse ScienceDirect

Journal of Asian Earth Sciences

journal homepage: www.elsevier.com/locate/jseaes

Analysis of site effects in magnetotelluric data by using the multifractal detrended fluctuation analysis

Luciano Telesca [a,*], Michele Lovallo [b], Han-Lun Hsu [c], Chien-Chih Chen [c]

[a] National Research Council, Institute of Methodologies for Environmental Analysis, C. da S. Loja, 85050 Tito (PZ), Italy
[b] ARPAB, Via della Fisica 18 C/D, 85100 Potenza, Italy
[c] Graduate Institute of Geophysics, National Central University, Jhongli 320, Taiwan, ROC

ARTICLE INFO

Article history:
Received 6 September 2011
Received in revised form 22 March 2012
Accepted 5 April 2012
Available online 20 April 2012

Keywords:
Magnetotellurics
Detrended fluctuation analysis

ABSTRACT

We investigated the multifractal structure of magnetic field H measured by magnetotelluric stations installed at three different sites in Taiwan, characterized by different site conditions. Magnetotelluric data include three components of the magnetic field H. We applied the multifractal detrended fluctuation analysis (MF-DFA) to magnetic magnitude time series (evaluated as the L^2 norm). Our findings point out to a significant discrimination among these data in terms of multifractal characteristics of the signals, indicating a strong influence of the environmental settings of the measurement sites on the temporal fluctuations of magnetic field H. Such results highlight the usefulness of the MF-DFA in discriminating dynamics in observational time series of magnetotellurics.

1. Introduction

Natural electromagnetic (EM) field in the Earth's sky is changed due to the solar wind and lightning activities and the secondary inductive EM wave is propagated in the solid Earth. The magnetotelluric (MT) method is a technique measuring the variation in the EM field on the Earth's surface for geological mapping of the subsurface structures (Chen and Chen, 1998; Chen et al., 2007). The MT data include two electric (E_x, E_y) and two magnetic (H_x, H_y) components, both in horizontal layouts with the north–south and east–west directions, and one vertical magnetic (H_z) component. The fundamental MT transfer function between the amplitudes of electric and magnetic fields can be written as $\mathbf{E}_i(\omega) = \mathbf{Z}_{ij}(\omega) * \mathbf{H}_j(\omega)$, where ω is the frequency and $\mathbf{Z}$ is the impedance tensor related to the electrical properties of subsurface materials. Except for the conventional MT processing algorithms, recently, several tools of nonlinear time series analysis have been applied on MT data for extracting quantitative dynamical properties (Telesca et al., 2006; Balasco et al., 2007, 2008).

The potential of multifractal analysis is far from being fully exploited, since it was only rather recently that attention has been drawn to the need for a thorough testing of the multifractal tools, and, in particular, a much deeper understanding of the nature of the seismic phenomena and their interactions with the multifractal methods used for their analysis (Telesca et al., 2001, 2002, 2004b, 2005b; Telesca and Lapenna, 2006).

Recently analyzing the multifractal properties of geoelectrical signals measured in seismic areas, it was found a significant correlation between variation of multifractal degree and earthquakes. In particular it was found that geoelectrical signals measured in seismic areas are characterized by a larger multifractal degree than that of geoelectrical signals measured in areas with low seismicity (Telesca et al., 2003, 2004a). Significant increase of multifractal degree in geoelectrical signals was detected before the occurrence of relatively large seismic events (Telesca et al., 2004c, 2005a,c). Ultra Low Frequency (ULF) magnetic signals measured in Crete (Greece) revealed their multifractality and significant difference between horizontal and vertical components (Telesca et al., 2004d). Volcano-magnetic signals were investigated by MF-DFA, showing that the multifractal spectrum of pre-eruptive phase is wider than that of post-eruptive phase (Currenti et al., 2005). From these results it can be argued the potential of multifractal methods in revealing dynamical characteristics in geophysical time series.

In this study, we analyzed the observed three magnetic channels of MT time series measured in Taiwan. In order to study the dynamics of these data, we used the multifractal detrended fluctuation analysis (MF-DFA). We clearly find that the multifractal behavior of the magnetic field is different in sites with different environmental conditions (e.g. oceanic- or landed-dominance).

2. Data description

The MT data analysed in this paper were continuously recorded with 15-Hz sampling rate by the MTU-5A systems (Phoenix Ltd., Canada) at three sites in Taiwan, indicated as 1871, 1878 and

* Corresponding author.
E-mail address: luciano.telesca@imaa.cnr.it (L. Telesca).

1367-9120/$ - see front matter © 2012 Elsevier Ltd. All rights reserved.
http://dx.doi.org/10.1016/j.jseaes.2012.04.002

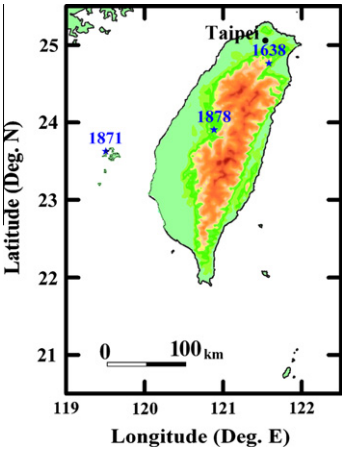

Fig. 1. Locations of MT observation sites (blue stars). (For interpretation of the references to color in this figure legend, the reader is referred to the web version of this article.)

1638 (Fig. 1). One site, 1871, is located in an area nearby the ocean, while the other two are located in areas relatively far from the ocean. The recording span is 1 week; the data were recorded at sites 1638 and 1878 from 5 September 2009 through 12 September 2009 and at site 1871 from 20 through 27 July 2009. We investigated the time dynamics of the 15-min averages of the three magnetic components at each site, for which the length scale of the penetration of the EM signal can approximate the crustal thickness. The possible difference between the three sites can also be due to the seasonal variation of the geomagnetic field (Yamazaki et al., 2011), but the long-period seasonal variation of geomagnetic field cannot be detected in our short-term records of 1 week.

3. Multifractal detrended fluctuation analysis

The main features of multifractals is to be characterized by high variability on a wide range of temporal or spatial scales, associated to intermittent fluctuations and long-range power-law correlations. The data examined in this paper present clear irregular dynamics (Fig. 2), characterized by fast fluctuations, which suggest to perform a multifractal analysis, in order to evidence different scaling behaviors for different intensities of fluctuations. We applied the multifractal detrended fluctuation analysis (MF-DFA), which operates on the series $x(i)$, where $i = 1,2,\ldots,N$ and N is the length of the series (Kantelhardt et al., 2002). With x_{ave} we indicate the mean value. We assume that $x(i)$ are increments of a random walk process around the average x_{ave}, thus the "trajectory" or "profile" is given by the integration of the signal

$$y(i) = \sum_{k=1}^{i} [x(k) - x_{ave}] \tag{1}$$

Next, the integrated series is divided into $N_S = \mathrm{int}(N/s)$ nonoverlapping segments of equal length s. Since the length N of the series is often not a multiple of the considered time scale s, a short part at the end of the profile $y(i)$ may remain. In order not to disregard this part of the series, the same procedure is repeated starting from the opposite end. Thereby, $2N_S$ segments are obtained altogether. Then we calculate the local polynomial trend for each of the $2N_S$ segments by a least square fit of the series. Then we determine the variance

$$F^2(s,v) = \frac{1}{s}\sum_{i=1}^{s}\{y[(v-1)s+i] - y_v(i)\}^2 \tag{2}$$

for each segment v, $v = 1,\ldots,N_S$ and

$$F^2(s,v) = \frac{1}{s}\sum_{i=1}^{s}\{y[N-(v-N_S)s+i] - y_v(i)\}^2 \tag{3}$$

for $v = N_S + 1,\ldots,2N_S$. Here, $y_v(i)$ is the fitting line in segment v. Then, we average over all segments to obtain the qth order fluctuation function

$$F_q(s) = \left\{\frac{1}{2N_S}\sum_{v=1}^{2N_S}[F^2(s,v)]^{\frac{q}{2}}\right\}^{\frac{1}{q}} \tag{4}$$

where in general, the index variable q can take any real value except zero. Repeating the procedure described above, for several time scales s, $F_q(s)$ will increase with increasing s. Then analyzing log–log plots $F_q(s)$ versus s for each value of q, we determine the scaling behavior of the fluctuation functions. If the series $x(i)$ is long-range power-law correlated, $F_q(s)$ increases for large values of s as a power-law

$$F_q(s) \approx s^{h_q} \tag{5}$$

The value h_0 corresponds to the limit h_q for $q \to 0$, and cannot be determined directly using the averaging procedure of Eq. (4) because of the diverging exponent. Instead, a logarithmic averaging procedure has to be employed,

$$F_0(s) \equiv \exp\left\{\frac{1}{4N_S}\sum_{v=1}^{2N_S}\ln[F^2(s,v)]\right\} \approx s^{h_0} \tag{6}$$

In general the exponent h_q will depend on q. We call h_q the generalized Hurst exponent (Kantelhardt et al., 2002). h_q independent of q characterizes monofractal series. The different scaling of small and large fluctuations will yield a significant dependence of h_q on q. For positive q, the segments v with large variance (i.e. large deviation from the corresponding fit) will dominate the average $F_q(s)$. Therefore, if q is positive, h_q describes the scaling behavior of the segments with large fluctuations; and generally, large fluctuations are characterized by a smaller scaling exponent h_q for multifractal time series. For negative q, the segments v with small variance will dominate the average $F_q(s)$. Thus, for negative q values, the scaling exponent h_q describes the scaling behavior of segments with small fluctuations, usually characterized by larger scaling exponents.

From the generalized Hurst exponent, we can derive the multifractal spectrum. On the base of the relationship

$$\tau_q = qh_q - 1 \tag{7}$$

and then the Legendre transform (Parisi and Frisch, 1985),

$$\alpha = \frac{d\tau}{dq} \tag{8}$$

$$F_\alpha = q\alpha - \tau_q \tag{9}$$

where α is the Hölder exponent and f_α indicates the dimension of the subset of the series that is characterized by α (Robertson et al., 2003).

4. Data analysis

We analysed the 1-week long 15-min averages of the magnitude of the magnetic field measured at three sites in Taiwan (labelled as station 1638, 1871 and 1878). The magnitude was calculated as the L^2 norm:

$$H_t = \sqrt{H_{t,x}^2 + H_{t,y}^2 + H_{t,z}^2} \tag{10}$$

where the subscript t indicates the station and x, y and z are the direction of the H component.

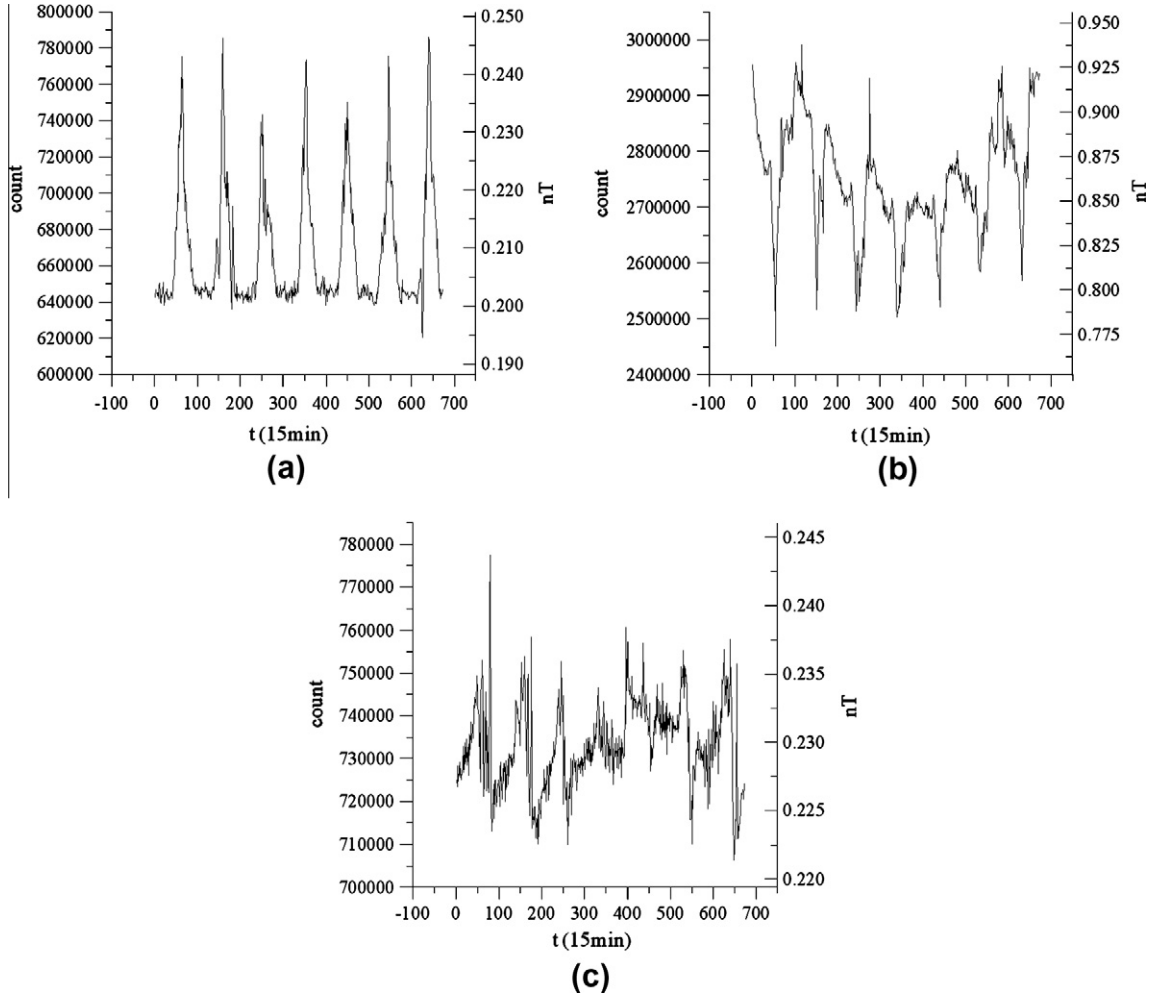

Fig. 2. Time variation of the H magnitude of the MT field at site 1871 (a), 1878 (b) and 1638 (c).

Fig. 2 shows the time variation of magnitude of the magnetic fields measured at the three stations. Most all the investigated variables have an oscillatory and spiky behavior, and this could affect the scaling behavior of the signals (Chen et al., 2002).

Let's examine the scaling behavior of H_{1871}. We applied the MF-DFA varying q from −5 to +5 and the scale s from 30 to $N/4$, being N the length of the series. Fig. 3 shows the fluctuation function $F_5(s)$, which is characterized by two scaling regimes separated by the crossover $s_c \sim 95$ that is the period of the spiky wave superimposed to the signal H_{1871}. The generalized Hurst exponent in the first regime is $h_5 \sim 0.95$. Fig. 4 shows the fluctuation function $F_{-5}(s)$; three different scaling regimes are clearly visible, separated by the

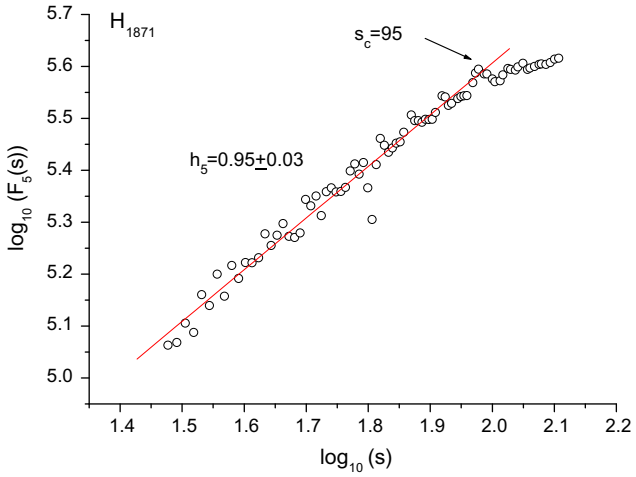

Fig. 3. Fluctuation function $F_5(s)$ for H_{1871}.

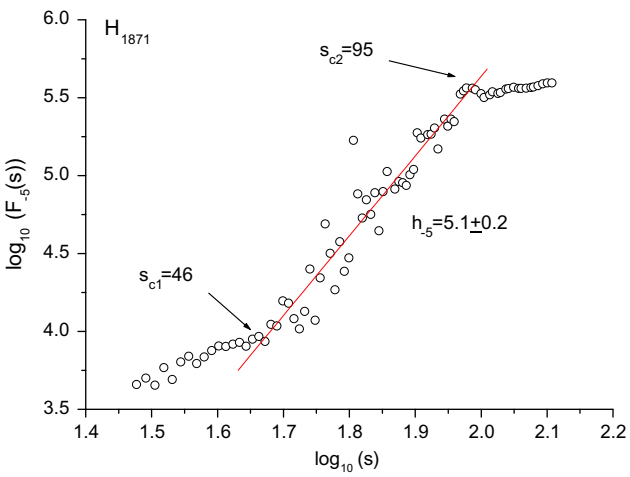

Fig. 4. Fluctuation function $F_{-5}(s)$ for H_{1871}.

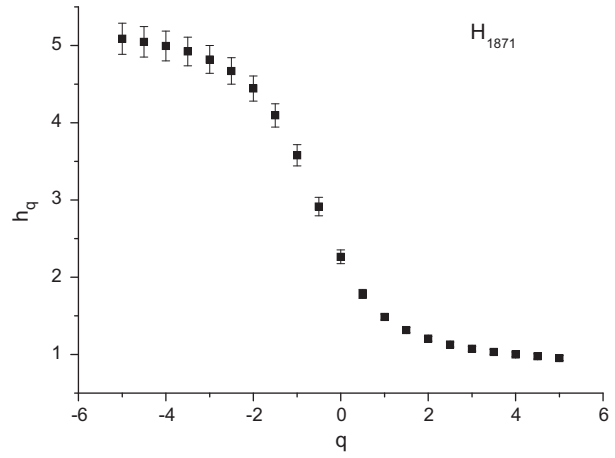

Fig. 5. Spectrum of generalized Hurst exponents for H_{1871}.

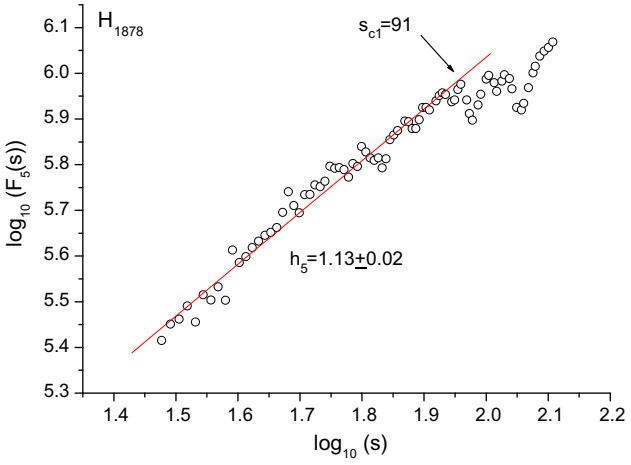

Fig. 6. Fluctuation function $F_5(s)$ for H_{1878}.

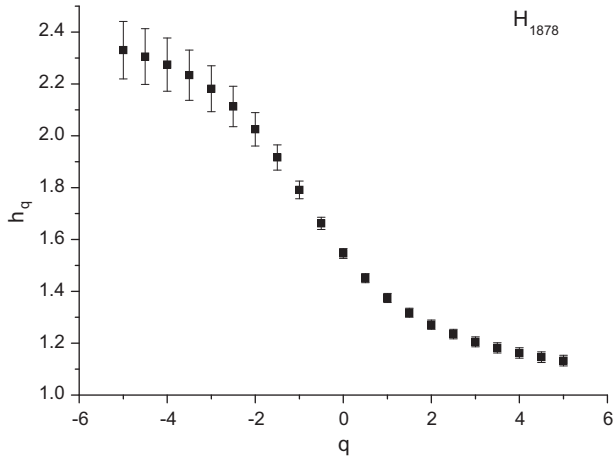

Fig. 7. Spectrum of generalized Hurst exponents for H_{1878}.

crossovers $s_{c1} \sim 46$ and $s_{c2} \sim 95$. The crossover s_{c1} is consistent with the average width of the spikes in the signal H_{1871}. The scaling exponent h_{-5} is calculated within the range delimited by the two crossovers and is about 5.1. It is clear that the scaling depends on the oscillatory spiky behavior of the signal, and, therefore, the generalized Hurst exponents for any q were estimated in the

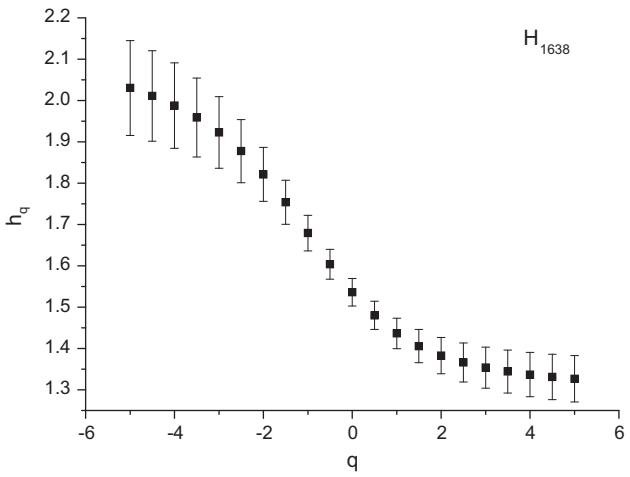

Fig. 8. Spectrum of generalized Hurst exponents for H_{1638}.

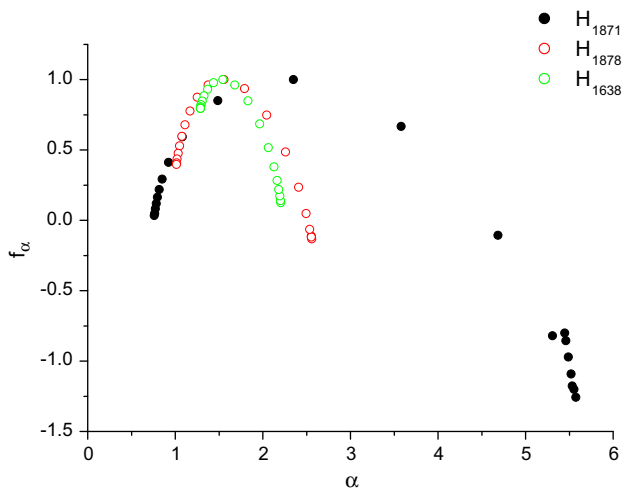

Fig. 9. Multifractal spectra.

scaling range between the two crossovers s_{c1} and s_{c2}. The results are shown in Fig. 5. The spectrum of the generalized Hurst exponent $h_q \sim q$ shows the typical multifractal behavior, with h_q monotonically decreasing with q.

Let's examine the multifractality of H_{1878}. Fig. 6 shows the fluctuation function $F_5(s) \sim s$. A crossover $s_{c1} \sim 91$ is consistent with the period of the spikes and the generalized Hurst exponent $h_5 \sim 1.13$. The generalized Hurst spectrum $h_q \sim q$ was, then, calculated for any q in the range $s < s_{c1}$ (Fig. 7).

Following the same approach, the generalized Hurst spectra for H_{1638} was calculated for any q in the range $s < s_{c1}$, with $s_{c1} = 67$ (Fig. 8).

Fig. 9 shows the multifractal spectra of the interevent times of the investigated seismicity and the quadratic fit. It is clearly evident that the width of the multifractal spectrum of H_{1871} is significantly larger than that of H_{1878} and H_{1638}.

In addition, we also applied conventional processing method of MT data and the resistivity-depth sections (Fig. 10) were computed at every sites by using the one-dimensional Occam inversion approach (Constable et al., 1987). The site 1871 contains a 1-km-thick layer with averagely 10-Ω m in the shallow crust, which is very much different from the other two sites. Such low resistivity should be caused by the ocean effect to our MT data or the in situ crustal basalts.

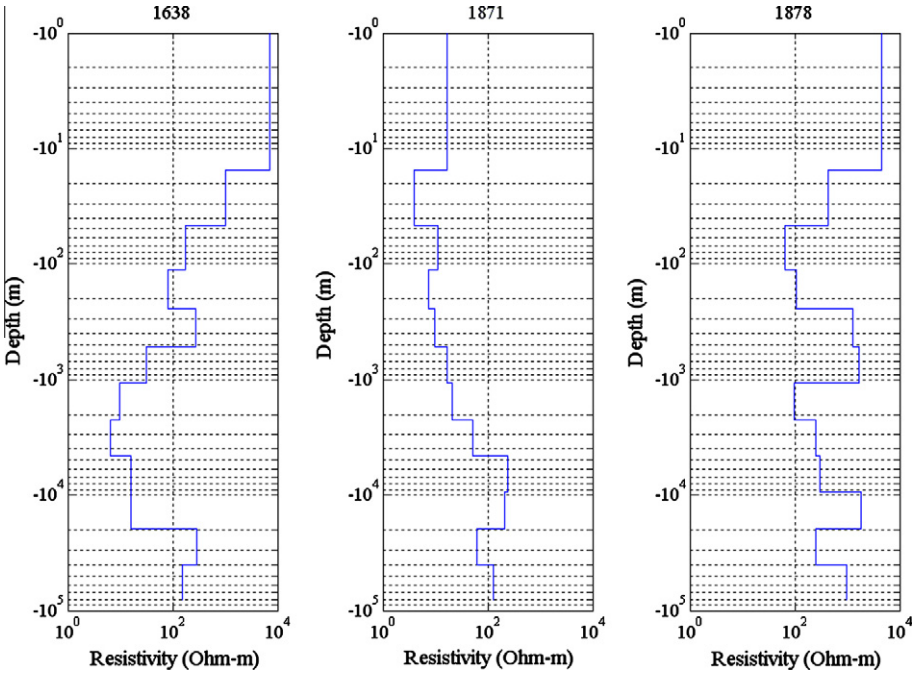

Fig. 10. 1D resistivity model of MT sites.

5. Discussion and conclusions

The results presented in this study show the multifractal nature of magnetic component of the MT filed measured in Taiwan. In particular, it has been shown that the degree of multifractality, which can be estimated by the width of the multifractal spectrum, is characterized by a visibly larger value for the magnetic signal measured in sites located in areas with relatively low seismic activity respect to the value of the width of the multifractal spectra of those magnetic signals recorded in areas with relatively very high seismic activity. The multifractality is an indication of the heterogeneity of the crust and could be presumably linked with the characteristic of the crustal seismogenic zones. The geology and environmental settings were much different between station 1871 and other sites on inland Taiwan (Angelier et al., 1990). Station 1871 is located at the basaltic area while the other two sites are located at the areas of sedimentary rocks with slight metamorphism. It is also however possible that the higher multifractal degree of the magnetic signal at station 1871 could be attributed to the hybrid effects of crustal and oceanic electrical circumstances. It is well-known to the MT community that parts of the long-period magnetic energies are generated from electrical currents carried by the oceanic brine currents (Chen and Chen, 1998; Chiang et al., 2010). Strong tidal effects in geoelectric potential field have been also found at the Nijima, Japan station (Huang and Liu, 2006). The lower resistivity at station 1871 (Fig. 10) may induce the stronger magnetic signal changed with the variation of magnetic filed. The signal H_{1871} may be thus included the stronger response of the EM induced from the ocean and igneous rocks.

Even if firm conclusions about the multifractal discrimination between MT magnetic signals measured in different geological settings should be further verified by using longer data sets recorded in more sites with different tectonic settings, it is, however, striking how the MF-DFA method is capable to extract quantitative information about the dynamics of such signals, which are obviously very complex. In any case, it is clearly evident that the multifractality is a feature for discriminating magnetic MT signals due to the site effects.

Acknowledgements

This study was supported by the Bilateral Project CNR-NSC 2012–2013 "Advanced time series analysis tools for magnetotelluric data". CCC acknowledges the NSC Grant 101-2923-M-008-003-MY2.

References

Angelier, J., Bergerat, F., Chu, H.T., Juang, W.S., Lu, C.Y., 1990. Paleostress analysis as a key to margin extension: the Penghu Islands, South China Sea. Tectonophysics 183, 161–176.

Balasco, M., Lapenna, V., Romano, G., Siniscalchi, A., Telesca, L., 2007. Extracting quantitative dynamics in Earth's apparent resistivity time series by using the detrended fluctuation analysis. Physica A 374, 380–388.

Balasco, M., Lapenna, V., Lovallo, M., Romano, G., Siniscalchi, A., Telesca, L., 2008. Fisher information measure analysis of Earth's apparent resistivity. Int. J. Nonlinear Sci. 5, 230–236.

Chen, C.C., Chen, C.S., 1998. Preliminary result of magnetotelluric soundings in the fold-thrust belt of Taiwan and possible detection of dehydration. Tectonophysics 292, 101–117.

Chen, Z., Ivanov, P.Ch., Hu, K., Stanley, H.E., 2002. Effect of nonstationarities on detrended fluctuation analysis. Phys. Rev. E 65, 041107.

Chen, C.C., Chi, S.C., Chen, C.S., Yang, C.H., 2007. Electrical structures of the source area of the 1999 Chi-Chi, Taiwan, earthquake: spatial correlation between crustal conductors and aftershocks. Tectonophysics 443, 280–288.

Chiang, C.W., Chen, C.C., Unsworth, M.J., Bertrand, E.A., Chen, C.S., Thong, K.D., Hsu, H.L., 2010. The deep electrical structure of southern Taiwan and its tectonic implications. Terr. Atmos. Ocean. Sci. 21, 879–895.

Constable, S.C., Parker, R.L., Constable, C.G., 1987. Occam's inversion: a practical algorithm for generating smooth models from electromagnetic sounding data. Geophysics 52, 289–300.

Currenti, G., Del Negro, C., Lapenna, V., Telesca, L., 2005. Multifractality in local geomagnetic field at Etna volcano, Sicily (southern Italy). Nat. Hazards Earth Syst. Sci. 5, 555–559.

Huang, Q., Liu, T., 2006. Earthquakes and tide response of geoelectric potential field at the Niijima station. Chin. J. Geophys. 49, 1585–1594.

Kantelhardt, J.W., Zschiegner, S.A., Konscienly-Bunde, E., Havlin, S., Bunde, A., Stanley, H.E., 2002. Multifractal detrended fluctuation analysis of nonstationary time series. Physica A 316, 87–114.

Parisi, G., Frisch, U., 1985. In: Ghil, M., Benzi, R., Parisi, G. (Eds.), Turbulence and Predictability in Geophysical Fluid Dynamics and Climate Dynamics. North Holland, Amsterdam.

Robertson, A.N., Farrar, C.R., Sohn, H., 2003. Singularity detection for structural health monitoring using holder exponents. Mech. Syst. Signal Process. 17, 1163–1184.

Telesca, L., Cuomo, V., Lapenna, V., Macchiato, M., 2001. Intermittent-type temporal fluctuations in seismicity of the Irpinia (southern Italy) region. Geophys. Res. Lett. 28, 3765–3768.

Telesca, L., Lapenna, V., Vallianatos, F., 2002. Monofractal and multifractal approaches in investigating scaling properties in temporal patterns of the 1983–2000 seismicity in the Western Corinth Graben (Greece). Phys. Earth Planet. Int. 131, 63–79.

Telesca, L., Colangelo, G., Lapenna, V., Macchiato, M., 2003. Monofractal and multifractal characterization of geoelectrical signals measured in southern Italy. Chaos, Solitons Fractals 18, 385–399.

Telesca, L., Balasco, M., Colangelo, G., Lapenna, V., Macchiato, M., 2004a. Investigating the multifractal properties of geoelectrical signals measured in southern Italy. Phys. Chem. Earth 29, 295–303.

Telesca, L., Lapenna, V., Macchiato, M., 2004b. Mono- and multi-fractal investigation of scaling properties in temporal patterns of seismic sequences. Chaos, Solitons Fractals 19, 1–15.

Telesca, L., Colangelo, G., Lapenna, V., Macchiato, M., 2004c. Fluctuation dynamics in geoelectrical data: an investigation by using multifractal detrended fluctuation analysis. Phys. Lett. A 332, 398–404.

Telesca, L., Lapenna, V., Vallianatos, F., Makris, J., Saltas, V., 2004d. Multifractal features in short-term time dynamics of ULF geomagnetic field measured in Crete, Greece. Chaos, Solitons Fractals 21, 273–282.

Telesca, L., Colangelo, G., Lapenna, V., 2005a. Multifractal variability in geoelectrical signals and correlations with seismicity: a study case in southern Italy. Nat. Hazards Earth Syst. Sci. 5, 673–677.

Telesca, L., Lapenna, V., Macchiato, M., 2005b. Multifractal fluctuations in seismic interspike series. Physica A 354, 629–640.

Telesca, L., Lapenna, V., Macchiato, M., 2005c. Multifractal fluctuations in earthquake-related geoelectrical signals. New J. Phys. 7, 214–228.

Telesca, L., Lapenna, V., 2006. Measuring multifractality in seismic sequences. Tectonophysics 423, 115–123.

Telesca, L., Balasco, M., Lapenna, V., Romano, G., Siniscalchi, A., 2006. Quantifying persistent behavior in Earth's apparent resistività time series. Fluctuat. Noise Lett. 6, L371–L378.

Yamazaki, Y., Yumoto, K., Cardinal, M.G., Fraser, B.J., Hattori, P., Kakinami, Y., Liu, J.Y., Lynn, K.J.W., Marshall, R., McNamara, D., Nagatsuma, T., Nikiforov, V.M., Otadoy, R.E., Ruhimat, M., Shevtsov, B.M., Shiokawa, K., Abe, S., Uozumi, T., Yoshikawa, A., 2011. An empirical model of the quiet daily geomagnetic field variation. J. Geophys. Res. 116, A10312. http://dx.doi.org/10.1029/2011JA016487.